



**AFRL-RH-WP-TR-2010-0140**

**Effect of Gold Nanorod Surface  
Chemistry on Cellular Interactions  
*In Vitro***

**Christin Grabinski  
Nicole Schaeublin  
Saber Hussain**

**711 HPW/RHPB  
2729 R Street  
Wright-Patterson AFB OH 45433-5707**

**September 2010**

**Interim report for Sep 09 to Sep 10**

Approved for public release;  
Distribution unlimited

**Air Force Research Laboratory  
711th Human Performance Wing  
Human Effectiveness Directorate  
Biosciences and Performance Division  
Applied Biotechnology Branch  
Wright-Patterson AFB OH 45433-5707**

## NOTICE

Using Government drawings, specifications, or other data included in this document for any purpose other than Government procurement does not in any way obligate the U.S. Government. The fact that the Government formulated or supplied the drawings, specifications, or other data does not license the holder or any other person or corporation; or convey any rights or permission to manufacture, use, or sell any patented invention that may relate to them.

This report was cleared for public release by the 88<sup>th</sup> Air Base Wing Public Affairs Office and is available to the general public, including foreign nationals. Copies may be obtained from the Defense Technical Information Center (DTIC) (<http://www.dtic.mil>).

**AFRL-RH-WP-TR-2010-0140**

THIS REPORT HAS BEEN REVIEWED AND IS APPROVED FOR PUBLICATION IN  
ACCORDANCE WITH ASSIGNED DISTRIBUTION STATEMENT.

//SIGNED//

SABER HUSSAIN, Work Unit Manager  
Applied Biotechnology Branch

//SIGNED//

MARK M. HOFFMAN, Deputy Chief  
Biosciences and Protection Division  
Human Effectiveness Directorate  
711th Human Performance Wing  
Air Force Research Laboratory

This report is published in the interest of scientific and technical information exchange, and its publication does not constitute the Government's approval or disapproval of its ideas or findings.

**REPORT DOCUMENTATION PAGE****Form Approved**  
**OMB No. 0704-0188**

Public reporting burden for this collection of information is estimated to average 1 hour per response, including the time for reviewing instructions, searching data sources, gathering and maintaining the data needed, and completing and reviewing the collection of information. Send comments regarding this burden estimate or any other aspect of this collection of information, including suggestions for reducing this burden to Washington Headquarters Service, Directorate for Information Operations and Reports, 1215 Jefferson Davis Highway, Suite 1204, Arlington, VA 22202-4302, and to the Office of Management and Budget, Paperwork Reduction Project (0704-0188) Washington, DC 20503.

**PLEASE DO NOT RETURN YOUR FORM TO THE ABOVE ADDRESS.**

<b>1. REPORT DATE (DD-MM-YYYY)</b> 9-27-10		<b>2. REPORT TYPE</b> Interim		<b>3. DATES COVERED (From - To)</b> Sep 09 – Sep 10	
<b>4. TITLE AND SUBTITLE</b> Effect of Gold Nanorod Surface Chemistry on Cellular Interactions In Vitro				<b>5a. CONTRACT NUMBER</b>	
				<b>5b. GRANT NUMBER</b> NA	
				<b>5c. PROGRAM ELEMENT NUMBER</b> 62202F	
<b>6. AUTHOR(S)</b> Christin Grabinski, Nicole Schaeublin, Saber Hussain				<b>5d. PROJECT NUMBER</b> OAF	
				<b>5e. TASK NUMBER</b> WP	
				<b>5f. WORK UNIT NUMBER</b> OAFWP004	
<b>7. PERFORMING ORGANIZATION NAME(S) AND ADDRESS(ES)</b> 711 HPW/RHPB, 2729 R Street, Wright-Patterson AFB OH 45433-5707				<b>8. PERFORMING ORGANIZATION REPORT NUMBER</b>	
<b>9. SPONSORING/MONITORING AGENCY NAME(S) AND ADDRESS(ES)</b> Air Force Materiel Command Air Force Research Laboratory 711 <sup>th</sup> Human Performance Wing Human Effectiveness Directorate Biosciences and Performance Division Applied Biotechnology Branch Wright Patterson AFB OH 45433-5707				<b>10. SPONSOR/MONITOR'S ACRONYM(S)</b> 711 HPW/RHPB	
				<b>11. SPONSORING/MONITORING AGENCY REPORT NUMBER</b>  AFRL-WP-RH-2010-0140	
<b>12. DISTRIBUTION AVAILABILITY STATEMENT</b> Approved for public release; distribution unlimited.					
<b>13. SUPPLEMENTARY NOTES</b> 88ABW cleared 12/9/10, 88ABW-2010-6459					
<b>14. ABSTRACT</b> Gold nanorods (GNRs) are of interest in many biological applications, including drug delivery and biomedical imaging due to their unique optical properties and the versatility for surface modification. For use in such applications, it is important to understand the effect of surface chemistry on the toxicological effects of GNRs to cells. In the current study, GNR stabilized with cetyltrimethylammonium bromide (GNR-CTAB) and GNR functionalized via a ligand exchange method with either thiolated polyethylene glycol (PEG) 5000 or mercaptohexadecanoic acid (MHDA) were investigated for their stability in biological media and toxicological effects to HaCat cells. Cell viability assays demonstrated minimal toxicity of GNR-PEG and GNR-MHDA and high toxicity of GNR-CTAB, which was found to be due to the inherent toxicity of the cationic surfactant to cells. Due to this high level of toxicity, further studies focused only on GNR-MHDA and GNR-PEG. Cell uptake studies indicated relatively low uptake for GNR-PEG and high uptake for GNR-MHDA. Reverse transcriptase polymerase chain reaction (RT-PCR) was used to determine effects at the genetic level and showed that GNR-PEG did not induce any effects, while GNR-MHDA influenced several of the genes investigated. Based on this information GNR-PEG is ideal for low cell uptake and high stability in biological media, while GNR-MHDA may be desirable for increased uptake of the GNRs into cells. However, further investigation into the potential effect of GNR-MHDA on gene expression is required.					
<b>15. SUBJECT TERMS</b> Nanorods      thiolated polyethylene glycol      mercaptohexadecanoic acid      gene expression					
<b>16. SECURITY CLASSIFICATION OF:</b>			<b>17. LIMITATION OF ABSTRACT</b>  SAR	<b>18. NUMBER OF PAGES</b>  29	<b>19a. NAME OF RESPONSIBLE PERSON</b> Saber Hussain
<b>a. REPORT</b> U	<b>b. ABSTRACT</b> U	<b>c. THIS PAGE</b> U			<b>19b. TELEPHONE NUMBER (Include area code)</b>

Standard Form 298 (Rev. 8-98)  
Prescribed by ANSI Std Z39-18

THIS PAGE INTENTIONALLY LEFT BLANK.

## TABLE of CONTENTS

List of Tables and Figures .....	iv
1. Abstract .....	1
2. Introduction and Background .....	1
3. Materials and Methods.....	4
3.1 GNR Synthesis and Functionalization .....	4
3.2 GNR Characterization.....	5
3.2 Cell Culture.....	5
3.3 GNR Stability in Biological Media.....	5
3.4 Biochemical Analysis.....	6
3.5 Cell Morphology and Uptake .....	7
3.6 Stress and Toxicity Array Analysis.....	8
4. Results and Discussion .....	9
4.1 GNR Characterization and Stability in Biological Media .....	9
4.2 Biochemical Analysis.....	11
4.3 Cell Morphology and Uptake .....	14
4.4 Stress and Toxicity Array Analysis .....	15
5. Summary and Conclusions.....	17
6. References .....	20
List of Symbols, Abbreviations, and Acronyms.....	22

## LIST OF TABLES

Table 1. TEM Characterization of GNR Size Distribution .....	9
Table 2. DLS Characterization of GNRs .....	9
Table 3. Genes Affected by Exposure to GNR-PEG and GNR-MHDA.....	17

## LIST OF FIGURES

Figure 1. TEM characterization of GNR morphology and size distribution .....	9
Figure 2. UV/VIS results for GNR-PEG and GNR-MHDA.....	10
Figure 3. Cell viability following a 24 h treatment with GNR-CTAB.....	11
Figure 4. Cell viability following a 2 h treatment with GNR-CTAB.....	12
Figure 5. Cell viability following a 24 h treatment with GNR-MHDA and GNR-PEG measured via MTS assay .....	12
Figure 6. Oxidative stress production after exposure to GNR-CTAB.....	13
Figure 7. Oxidative stress production after exposure to GNR-MHDA and GNR-PEG .....	14
Figure 8. Cell uptake of GNR-MHDA and GNR-PEG in HaCat cells via DF imaging and TEM.....	15

## **1. ABSTRACT**

Gold nanorods (GNRs) are of interest in many biological applications, including drug delivery and biomedical imaging due to their unique optical properties and the versatility for surface modification. For use in such applications, it is important to understand the effect of surface chemistry on the toxicological effects of GNRs to cells. In the current study, GNR stabilized with cetyltrimethylammonium bromide (CTAB) and GNR functionalized via a ligand exchange method with either thiolated polyethylene glycol (PEG) 5000 or mercaptohexadecanoic acid (MHDA) were investigated for their stability in biological media and toxicological effects to HaCat cells. GNR-PEG and GNR-MHDA exhibited minimal effects on cell viability, whereas GNR-CTAB reduced cell viability significantly due to the inherent toxicity of the cationic surfactant to cells. As a result of this high level of toxicity, further studies focused only on GNR-MHDA and GNR-PEG. Cell uptake studies indicated relatively low uptake for GNR-PEG and high uptake for GNR-MHDA. Reverse transcriptase polymerase chain reaction (RT-PCR) revealed that GNR-PEG did not induce any significant changes in the transcription levels of 84 genes related to stress and toxicity, while GNR-MHDA influenced the transcription levels of several of the genes investigated. Based on this information, GNR-PEG is ideal for low cell uptake and high stability in biological media, while GNR-MHDA may be desirable for increased uptake of the GNRs into cells. However, further investigation into the potential effect of GNR-MHDA on gene expression is required.

## **2. INTRODUCTION AND BACKGROUND**

Gold nanorods (GNRs) are of interest in many biological applications, including photothermal therapy for gene/drug delivery (Huang et al., 2006; Wijaya et al., 2007), disease targeting (Chen et al., 2006), and medical/biological imaging (Agarwal et al., 2007). By changing the aspect ratio (AR) of GNRs, the plasmon peak absorption and scattering wavelength can be tuned to near infrared (NIR: 700–900 nm). This allows for photothermal applications via laser irradiation at the wavelength for longitudinal absorption and increased penetration depth into biological

tissue for biological imaging and contrast enhancement. Additionally, the surface of GNRs can be modified via thiol chemistry, which allows for specific biological targeting applications.

While GNRs have been demonstrated for use in many applications, it is important to understand the structure/activity effects of different physical and chemical properties of GNRs on cells. Previous studies on the cytotoxicity of various nanoparticles indicated that surface chemistry has a strong influence on cell toxicity and uptake (Hussain et al., 2009; Carlson et al., 2008; Niidome et al., 2006; Huff et al., 2007; Chithrani et al., 2006; Alkilany et al., 2009; Hauck et al., 2008; Mahonar et al., 2010). The surfactant cetyltrimethylammonium bromide (CTAB) is inherently present as a byproduct of GNR synthesis and has been shown to exhibit significant cytotoxicity (Alkilany et al., 09, Manohar et al., 09; Parab et al., 09; Leonov et al., 08).

Several surface coatings and chemically bonded functional groups have been proposed in order to reduce the apparent toxic effect of the surfactants such as CTAB. GNRs coated with polyacrylic acid (PAA), polyelectrolyte poly(allylamine) hydrochloride (PAH), and poly(4-styrene sulfonic acid) (PSS) and were found to be less toxic than GNR-CTAB (Alkilany et al., 2009; Hauck et al. 2008; Wang et al., 2008). When PSS-coated GNRs were further coated by poly(diallyldimethyl ammonium chloride) (PDADMAC), this particle was found to exhibit less cytotoxicity than GNR-CTAB. However, it was found that when GNRs were exposed to serum proteins before cells, GNR-CTAB become less toxic and those with a surface composition of PDADMAC become more toxic. Thus, the initial surface composition of GNRs may determine which proteins are adsorbed onto the surface, thereby effecting toxicity (Hauck et al. 2008).

This effect has also been demonstrated in the case of cell uptake (Alkilany et al., 2009). In a study using HT-29 cells, it was found that after coating positively charged CTAB with negatively charged polymer PAA, followed by a positively charged polymer PAH, cell uptake was dramatically improved for PAH as the outermost coat versus PAA as determined by inductively coupled plasma – mass spectrometry (ICP-MS). However, all GNR samples exhibited very similar surface charge (zeta potential = -20 mV) when dispersed in cell culture media (before cellular exposure), suggesting that proteins adsorbed onto GNR surface. This also indicates a



complex relationship between surface charge of the GNR before and after protein adsorption and how cell uptake is affected (Alkilany et al., 2009).

In a similar study, HeLa cells were exposed to GNRs coated with CTAB, CTAB-PSS, CTAB-PSS-PDADMAC, CTAB-PSS-PDADMAC-PSS after exposure to serum proteins. CTAB-PSS (zeta potential = -69.5 mV) exhibited the lowest cell uptake and CTAB-PSS-PDADMAC (zeta potential = +37.1 mV) had highest cell uptake as determined by ICP- atomic emission spectroscopy (AES). GNRs coated with CTAB-PSS-PDADMAC-PSS (zeta potential = -35.1 mV) had intermediate cellular uptake. The results from this study demonstrate the crucial relationship between zeta potential and cell uptake (Hauck et al., 2008).

Studies have found that GNRs functionalized with polyethylene glycol (PEG) are more inert than other coatings (Niidome et al., 2006; Mahonar et al., 2010; Rayavarapu et al., 2010). In a study using the SKBR 3 (mammary adenocarcinoma) cell-line, thiolated PEG functionalized GNRs were found to be significantly less toxic (via MTS assay) than GNRs before and after filtering to remove excess CTAB in solution (Manohar et al., 2010). This same effect was found in a different study using HeLa cells and the MTT assay (Niidome et al., 2006).

Thiolated PEG functionalized GNRs were also found to be more biocompatible than PSS-coated GNRs in SKBR3 (mammary adenocarcinoma), CHO (Chinese Hamster Ovary), C2C12 (mouse myoblast), and HL60 (Human Leukemia) cell-lines using MTS assay (Rayavarapu et al., 2010). These studies show complete cell death for GNR-CTAB before and after filtration for all cell-lines. GNR-PSS also exhibited increased cytotoxicity compared to GNR-PEG, which was suggested to be a result of remaining CTAB on the surface, since PSS does not actually replace CTAB like PEG.

In addition to increased biocompatibility, PEGylated GNRs have shown significantly reduced cell uptake as compared with GNRs modified with other surface chemistries (Huff et al., 2007; Rayavarapu et al., 2010). A study using KB cells (tumor line derived from oral epithelium) found that GNRs coated with CTAB had 20 times the amount of cell uptake than those coated with PEG-DTC (dithiocarbamate) without incubation with serum proteins (Huff et al., 2006). A

similar effect was found in a study using SKBR3 (mammary adenocarcinoma) cells, which qualitatively found no cell uptake of GNR-PEG compared to GNRs coated with PSS (Rayavarapu et al., 2010).

When investigated *in vivo*, it was found that following injection of GNR-PEG (zeta potential =  $-0.5 \pm 0.4$  mV) and GNR-CTAB (zeta potential =  $+41 \pm 1$  mV) into mice, amounts of gold in blood, liver, lung, spleen, and kidney were quantified at different time points using ICP-MS. PEG functionalized GNRs took longer to leave the blood and accumulate in the kidney than those stabilized in CTAB (72 h and 0.5 h, respectively) (Niidome et al., 2006). This indicates that GNR-PEG not only exhibits reduced uptake into cells, but also takes longer for the body to recognize as a foreign material.

For the current study, three GNR samples were prepared by Dr. Hamad-Schifferli and colleagues at the Massachusetts Institute of Technology in order to further investigate the effect of surface chemistry on GNR interaction with cells. One sample is stabilized with CTAB and two are functionalized via a ligand exchange method with either thiolated PEG 5000 or mercaptohexadecanoic acid (MHDA) as previously described (Wijaya and Hamad-Schifferli, 2008). The goal of this study is to evaluate the relative toxic effect of GNRs to HaCat cells *in vitro* as a function of surface chemistry. HaCat cells were chosen as a representative model for dermal toxicity. Endpoints include stability in biological media via dynamic light scattering (DLS), UV/VIS, and darkfield (DF) microscopy. Cell viability and function were assayed via mitochondrial activity (MTS), membrane leakage (LDH), and oxidative stress (ROS) assays. Cell morphology and uptake were investigated using DF & fluorescence microscopy, as well as transmission electron microscopy (TEM). Reverse transcriptase polymerase chain reaction (RT-PCR) was used to investigate the effects of gene expression for GNR-MHDA and GNR-PEG.

### **3. MATERIALS AND METHODS**

#### **3.1 GNR Synthesis and Functionalization**

GNRs were synthesized by Kimberly Hamad-Schifferli's group using the seed-mediated growth method (Sau and Murphy, 2004). The CTAB surfactant on the GNR surface was replaced with PEG or MHDA by round-trip phase transfer ligand exchange as described in detail in Wijaya et al., 2008.

### **3.2 GNR Characterization**

To visualize the structure and size of the GNRs, a drop of the stock for each sample was placed on a TEM grid and viewed using a Hitachi H-7600 microscope at 100kV. The length and width were averaged for 100 particles measured using ImageJ software (NIH).

The concentration of stock solutions was determined using UV/VIS. The molar concentration of the GNR samples was calculated based on the Beer-Lambert Law using an extinction coefficient of  $4.6 \times 10^9 \text{ M}^{-1} \text{ cm}^{-1}$  at 800 nm. This result was multiplied by the dilution factor to yield the final molar concentration. To convert molar concentration to mass concentration, it was assumed that the GNRs exhibit a cylindrical shape with dimensions of 11 nm in diameter and 44 nm in length, and demonstrate a density of  $19.30 \text{ g/cm}^3$ .

### **3.3 Cell Culture**

The human keratinocyte cell line (HaCaT) was generously donated by the Army Research Lab. The cells were cultured in a flask with RPMI-1640 media (ATCC) supplemented with 10% fetal bovine serum (FBS, ATCC) and 1% penicillin/streptomycin (pen/strep, Sigma). For nanoparticle exposure, media was supplemented with 1% penicillin/streptomycin but no serum and was labeled as the exposure media (EM). Cells were incubated at 37°C in a humidified incubator with 5% CO<sub>2</sub>.

### **3.4 Stability of GNRs in Biological Media**

The relative stability of each GNR sample was determined after dispersion in water or EM using UV/VIS, DLS, and DF microscopy. For these studies, GNRs were suspended at a concentration of 100 µg/mL in water or EM and vortexed 30 seconds upon dilution and again immediately

before analysis. Samples were analyzed within 1 h of dilution. UV/VIS measurements were performed using a Varian Cary Bio 300 UV/VIS Spectrophotometer. A Malvern Zetasizer was used for DLS measurements of hydrodynamic diameter and also for zeta potential analysis of GNRs dispersed in water. For DF imaging, a small volume of this sample was spotted on a microscope slide and allowed to dry in air. Imaging was performed using a DF condenser from CytoViva attached to an Olympus BX41 microscope and DAGE camera/software.

### **3.5 Biochemical Analysis**

For biochemical assays, cells were seeded in a 96 well plate at a concentration of  $1.5 \times 10^5$  cells/cm<sup>2</sup> and allowed to proliferate and adhere for 24 h. Cells were dosed with varying concentrations of GNRs (5, 50, and 100 µg/mL) in media without serum (EM). The addition of EM to cells served as negative controls. Biochemical assays were initiated after a 24 h exposure and included the MTS, LDH, and ROS assays.

The MTS assay was performed using the CellTiter 96 Aqueous One Solution Cell Proliferation Assay (Promega). The solution reagent contains a tetrazolium compound [3-(4, 5-dimethylthiazol-2-yl)-5-(3-carboxymethoxyphenyl)-2-(4-sulfophenyl)-2H-tetrazolium, inner salt; MTS] and an electron coupling reagent (phenazine ethosulfate; PES). Metabolically active cells reduce the MTS compound into a colored formazan product that is soluble in tissue culture medium and can be measured using a standard microplate reader. After 24 h, the supernatant containing GNRs was aspirated from the wells and the cells were washed 3X with 1X PBS to remove residual GNRs. Mitochondrial function was then assessed according to the manufacturer's instructions.

Lactase dehydrogenase leakage (LDH) was evaluated to determine the integrity of the cell membrane using the used the CytoTox 96 Non-Radioactive Cytotoxicity Assay (Promega, Madison, WI). This is a colorimetric assay that quantitatively measures LDH, a stable cytosolic enzyme that is released upon cell lysis. Released LDH in culture supernatants is measured with a 30-min coupled enzymatic assay that results in the conversion of a tetrazolium salt into a red formazan product. For both the MTS and LDH assay, the formazan product was measured by

the amount of absorbance at 490 nm with a standard microplate reader (SpectraMAX GeminiXS, Molecular Devices, Sunnyvale, CA). The absorbance is directly proportional to the number of metabolically active cells and the number of lysed cells in the MTS and LDH assays, respectively. The spectrophotometer was calibrated to zero absorbance using EM without cells and a background reading was taken immediately after the addition of reagent to eliminate interference due to slight absorbance of GNRs near 490 nm.

In order to further investigate oxidative stress as a mechanism of cytotoxicity, the reactive oxygen species (ROS) assay was performed using the BD Pathway Confocal Microscope, which collects images and corresponding fluorescence intensity data. The generation of ROS was probed with the Image IT Live Green ROS detection kit (Molecular Probe, Invitrogen, Carlsbad, CA). This assay is based on a fluorescent marker for ROS in live cells (5-carboxy-22,72-dichlorodihydrofluoresceine diacetate; carboxy-H<sub>2</sub>DCFDA). The oxidation product of carboxy-H<sub>2</sub>DCFDA has excitation/emission maxima of approximately 495/529 nm. As a positive control, 0.03 % of hydrogen peroxide was added for 1 h to induce cellular apoptosis. After incubation, the cells were washed with warm PBS, then the monolayers were covered with the working solutions (Carboxy DCFA for ROS staining: 25  $\mu$ M; Hoechst solution for nuclear staining: 1  $\mu$ M). The cells were incubated at 37°C for 30 minutes, protected from light to avoid bleaching of the fluorophores. After rinsing with PBS, the cells were observed with DAPI and Fluorescein/FITC filters and fluorescence intensity for each was averaged for the pixels in each image. The results were presented in the form of fold change in fluorescence intensity of FITC/DAPI from control.

For each biochemical assay, three trials were performed for each sample with a value of n=3 per trial for a total of 9 data points for each sample. Statistical significance from control was determined for biochemical data using a two tailed t-test in Excel with p<0.05.

### **3.6 Cell Morphology and Uptake**

The interaction of GNR-MHDA and GNR-PEG cells was determined using DF imaging and transmission electron microscopy (TEM). For DF imaging, cells were plated in 2-chambered slides (surface area = 4 cm<sup>2</sup>) at a concentration of  $1.0 \times 10^5$  cells/cm<sup>2</sup> and allowed to proliferate

and adhere for 24-48 h or until ~80% confluent. For DF imaging experiments with GNR-MHDA and GNR-PEG, cells were dosed with GNRs diluted in EM at a concentration of 10 µg/mL and exposed for 24 h. Following exposure, cells were washed with PBS and fixed in 4% paraformaldehyde for 10 minutes. The cells were washed again with PBS, a coverslip was added and sealed with clear nail polish, and the slide was imaged using the CytoViva Hyperspectral Imaging System attached to an Olympus BX41 microscope (Aetos Technologies, Inc., Auburn, AL). Data was collected using ENVI software.

For TEM imaging, cells were seeded at a concentration of  $1.0 \times 10^5$  cells/cm<sup>2</sup> in 6-well plates (surface area = 9.6 cm<sup>2</sup>) and allowed to adhere and proliferate for 48 h. Cells were dosed with GNRs diluted in EM at a concentration of 50 µg/mL and exposed for 24 h. At the completion of the exposure period, cells were washed with PBS, trypsinized from the plate, and centrifuged at 1000xg for 10 minutes. The pellet was fixed in 2% paraformaldehyde overnight at 4°C. The following day, the cell pellets were washed with PBS, stained with 4% osmium tetroxide, and dehydrated with ethanol in a standard dilution sequence. The final pellet was cured in a vacuum oven using LR White resin (EMS) at 60°C. The cured sample was sectioned using a Leica EM UC6 Ultramicrotome and imaged using a Hitachi H-7600 TEM by Karl Strieker at the University of Dayton.

### **3.7 Gene Expression Analysis**

Reverse Transcription Polymerase Chain Reaction (RT-PCR) was used to determine the effect of GNR-MHDA and GNR-PEG exposure on HaCat cells at non-toxic doses (50 µg/mL). Cells were seeded and exposed to GNRs as described for TEM imaging. After 24 h exposure, RNA was isolated from the cells using a RNA Isolation Kit from Qiagen. The RNA yield was determined using the NanoDrop Spectrophotometer (ThermoScientific). Once RNA was successfully isolated from the cells, c-DNA was prepared using the RT<sup>2</sup> First Strand kit (SABiosciences) according to manufacturer's instructions. The Stress and Toxicity Array (SABiosciences) was used to evaluate the expression of 84 genes related to stress and toxicity production in human cells. Expression of genes that are directly regulated by oxidative or metabolic stress and heat shock, as well as

genes which are representative of pathways activated by prolonged stress, such as apoptosis and senescence are among those evaluated in this array. Three trials were performed for each sample (control, GNR-MHDA, and GNR-PEG).

## 4. RESULTS AND DISCUSSION

### 4.1 Characterization of GNRs and Stability in Biological Media

TEM was used to characterize the morphology and size distribution of GNRs, and ImageJ was used to measure and calculate the average length and width of each GNR sample. The morphology for all GNR samples is roughly cylindrical with a small amount of spheres. GNR-MHDA and GNR-PEG exhibit slightly larger size distribution than GNR-CTAB (figure 1, Table 1).

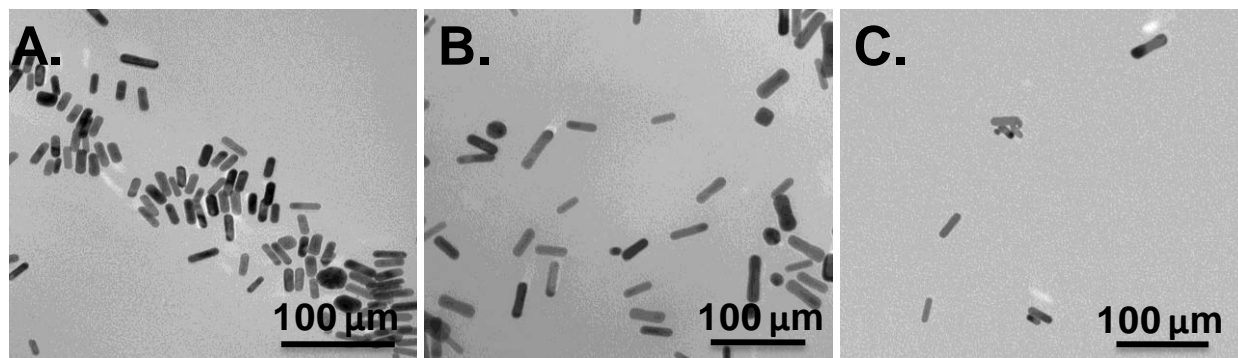


Figure 1. TEM characterization of GNR morphology and size distribution. A. GNR-CTAB; B. GNR-MHDA; C. GNR-PEG.

Table 1. TEM Characterization of GNR Size Distribution.

Sample	GNR-CTAB	GNR-MHDA	GNR-PEG
Average Length (nm)	25.6±3.6	35.5±8.9	31.7±9.6
Average Width (nm)	8.2±1.1	10.1±2.8	9.1±3.2
Aspect Ratio (AR)	3.1	3.5	3.5

DLS was used to determine the hydrodynamic diameter and zeta potential for each sample. GNR-CTAB and GNR-MHDA exhibit a hydrodynamic diameter close to 15 nm, which is likely due to the presence of surfactant molecules in solution. GNR-PEG exhibited a zeta potential value closest to neutral (-11.1 mV), while GNR-CTAB and GNR-MHDA exhibit zeta potential values at -44.5 mV and -46.2 mV, respectively. DLS values indicate significant agglomeration of GNR-MHDA and little agglomeration of GNR-PEG in EM. The polydispersity index (pdl) indicates on a scale of 0 to 1 the polydispersity of the sample, where a value of 0 is the minimum. Values close to 0.5 indicate a high level of polydispersity, which is expected for non-spherical particles (Table 2).

Table 2. DLS Characterization of GNRs.

Sample	Dispersant	Zeta Potential (mV)	Hydrodynamic Diameter (nm)	Pdl
GNR-CTAB	Water	+44.5 $\pm$ 0.354	14.2	0.627
	Media	NA	NA	NA
GNR-MHDA	Water	-46.2 $\pm$ 0.354	16.5	0.564
	Media	NA	1690.0	0.499
GNR-PEG	Water	-11.1 $\pm$ 0.989	40.3	0.476
	Media	NA	49.6	0.476

UV-VIS data and DF images confirm that GNR-PEG exhibit increased stability in media versus GNR-MHDA. GNR-MHDA shows a loss in the longitudinal peak (peak 2), indicating agglomeration. Darkfield images also show an increase in the size of the particles and reduced background containing individual GNRs (Figure 2).



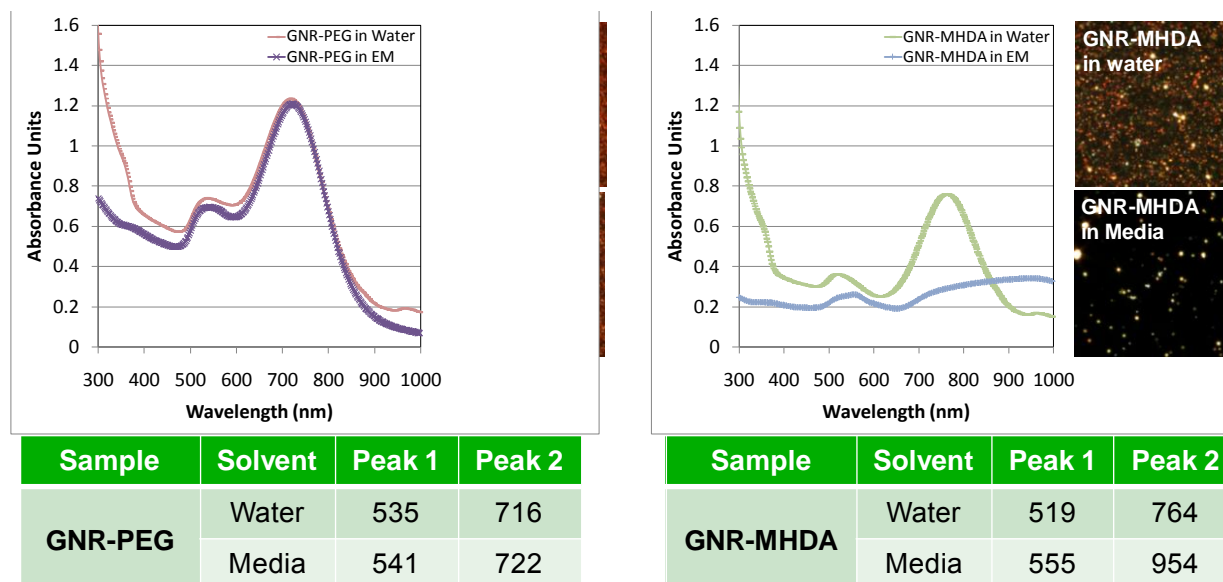


Figure 2. UV/VIS results for GNR-PEG and GNR-MHDA. Peak 1 represents the transverse absorption peak and peak 2 represents the longitudinal absorbance peak. DF images of GNRs in water and media are shown in insets.

## 4.2 Biochemical Analysis

MTS cell viability assays was performed to determine the effect of 24 h exposure to these particles on HaCat cells. After a 24 h exposure, GNR-CTAB reduced cell proliferation below 20% from control at all concentrations indicating it is highly toxic, and that there is not a dose-dependent response. A similar response was shown by the CTAB alone, so the CTAB itself is likely responsible for the GNR toxicity (Figure 3A). For GNR-CTAB, LDH leakage assay was performed to verify results from the MTS assay (Figure 3B). There were high levels of membrane leakage at the lower doses but at the higher doses there was not leakage. This is most likely caused by the higher doses having a cytotoxic effect earlier than the lower doses and the LDH is no longer in the media or is not produced by the cells. A similar trend was observed with the CTAB alone (Figure 3B).

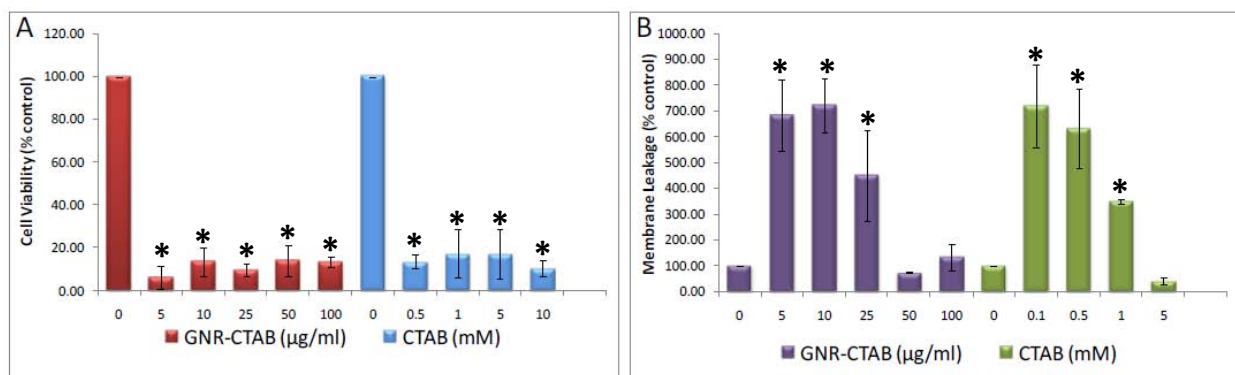


Figure 3. Cell viability following a 24 h treatment with GNR-CTAB. A. MTS assay; B. LDH assay. Error bars indicate standard deviation, the asterisk denotes significant toxicity.

The MTS and LDH assays were repeated at a shorter time-point to determine whether LDH leakage could be observed for the higher doses at a shorter time point. GNR-CTAB disrupted cell proliferation at all concentrations, thereby indicating that the cytotoxic effect occurs early and that it is not a dose-dependent response. Again, a similar trend was observed with the CTAB (Figure 4).

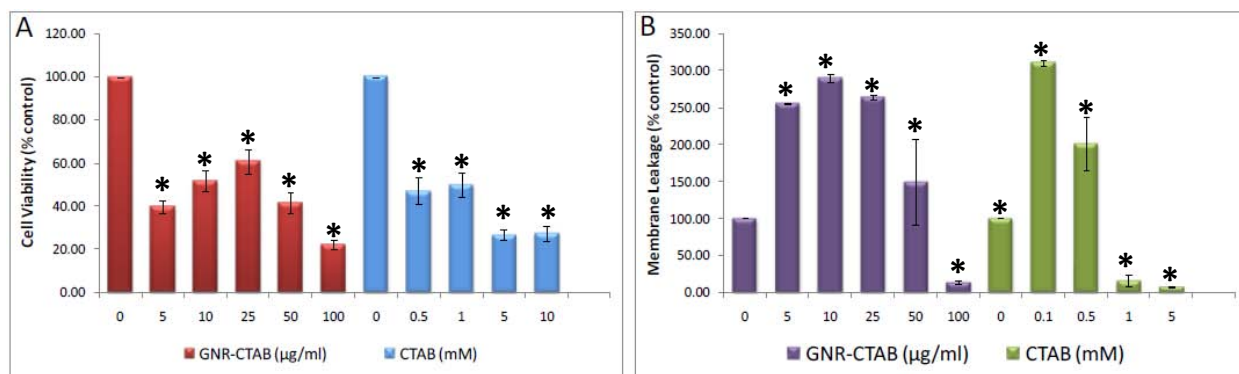


Figure 4. Cell viability following a 2 h treatment with GNR-CTAB. A. MTS assay; B. LDH assay. Error bars indicate standard deviation, the asterisk denotes significant toxicity.

The MTS assay was carried out for GNR-PEG and GNR-MHDA after a 24 h exposure to determine any effect on cell viability. GNR-MHDA increased cell proliferation at 5  $\mu\text{g/mL}$ , and GNR-MHDA and GNR-PEG showed significant decrease in cell viability at 100  $\mu\text{g/mL}$  (Figure 5).

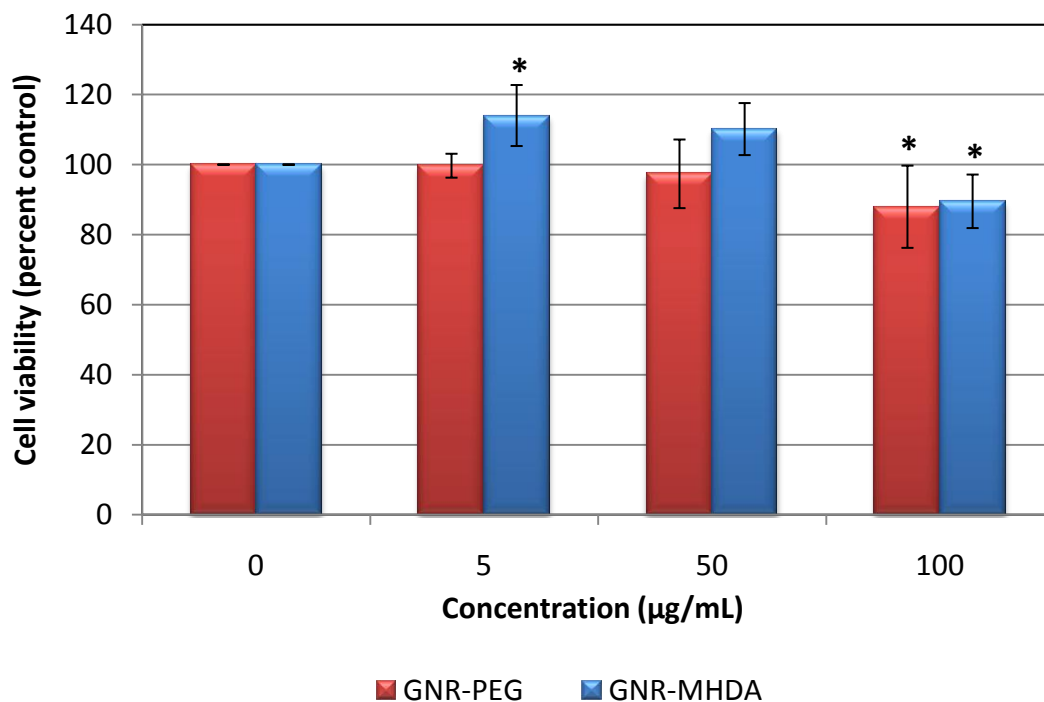


Figure 5. Cell viability following a 24 h treatment with GNR-MHDA and GNR-PEG measured via MTS assay. Asterisk denotes significance ( $p < 0.05$ ).

The ROS assay was performed to determine the oxidative stress response to cells exposed to GNRs. Qualitative data shows elevated production of ROS in cells exposed to GNR-CTAB (Figure 6). The negative control cells show no ROS production as expected, while the positive control cells show ROS formation.

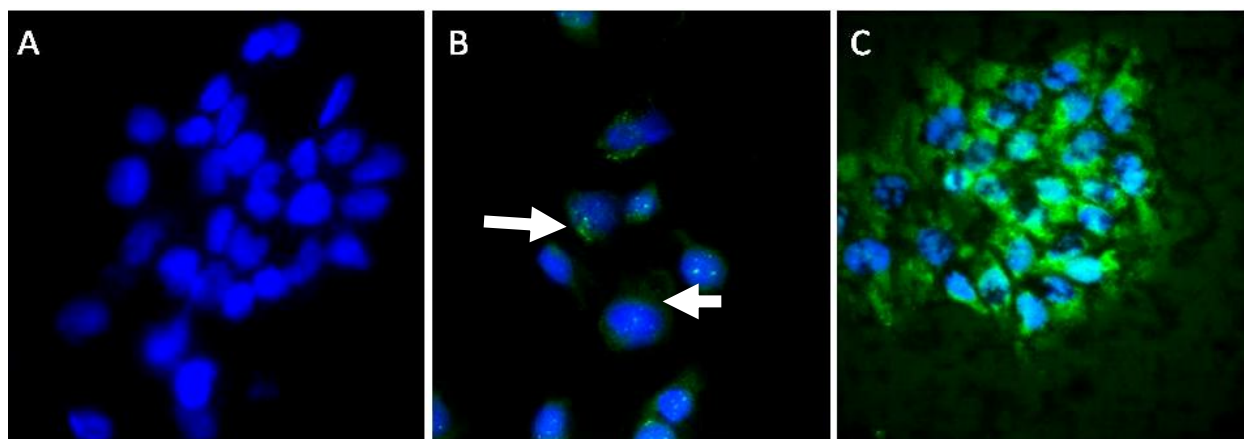


Figure 6. Oxidative stress production after exposure to GNR-CTAB. A. Negative control; B. Positive control (0.03% H<sub>2</sub>O<sub>2</sub>); C. 5 µg/ml GNR-CTAB. Nuclei are stained with Hoescht and the DCFH probe fluoresces green in the presence of ROS. White arrows indicate green fluorescence produced in positive control.

Quantitative ROS data was collected for GNR-MHDA and GNR-PEG in order to elucidate small differences in ROS production versus control cells. Neither GNR-MHDA nor GNR-PEG induced significant ROS after exposure (Figure 7).

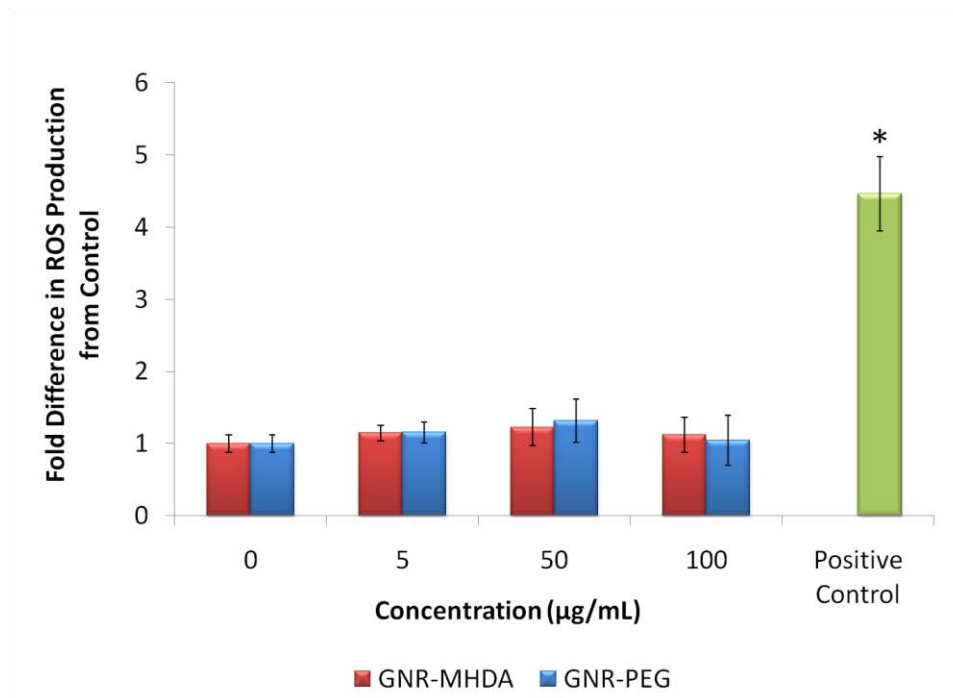


Figure 7. Oxidative stress production after exposure to GNR-MHDA and GNR-PEG. Data were normalized FITC intensity to Hoescht intensity to account for cell number.

### 4.3 Cell Morphology and Uptake

DF images indicate a high level of association of GNR-PEG with cells at the 24 h time point. However, after cell sectioning, only a minimal amount of cell uptake is observed (Figure 8). GNR-MHDA appear to have been taken up via endocytosis and are localized in endosomes within the cell. Based on the size of the endosomes (~0.5 µm) and the extensions on the surface

of the cell, it is likely that the mechanism of uptake is macropinocytosis, which directs the endosomes to the lysosomes for digestion.

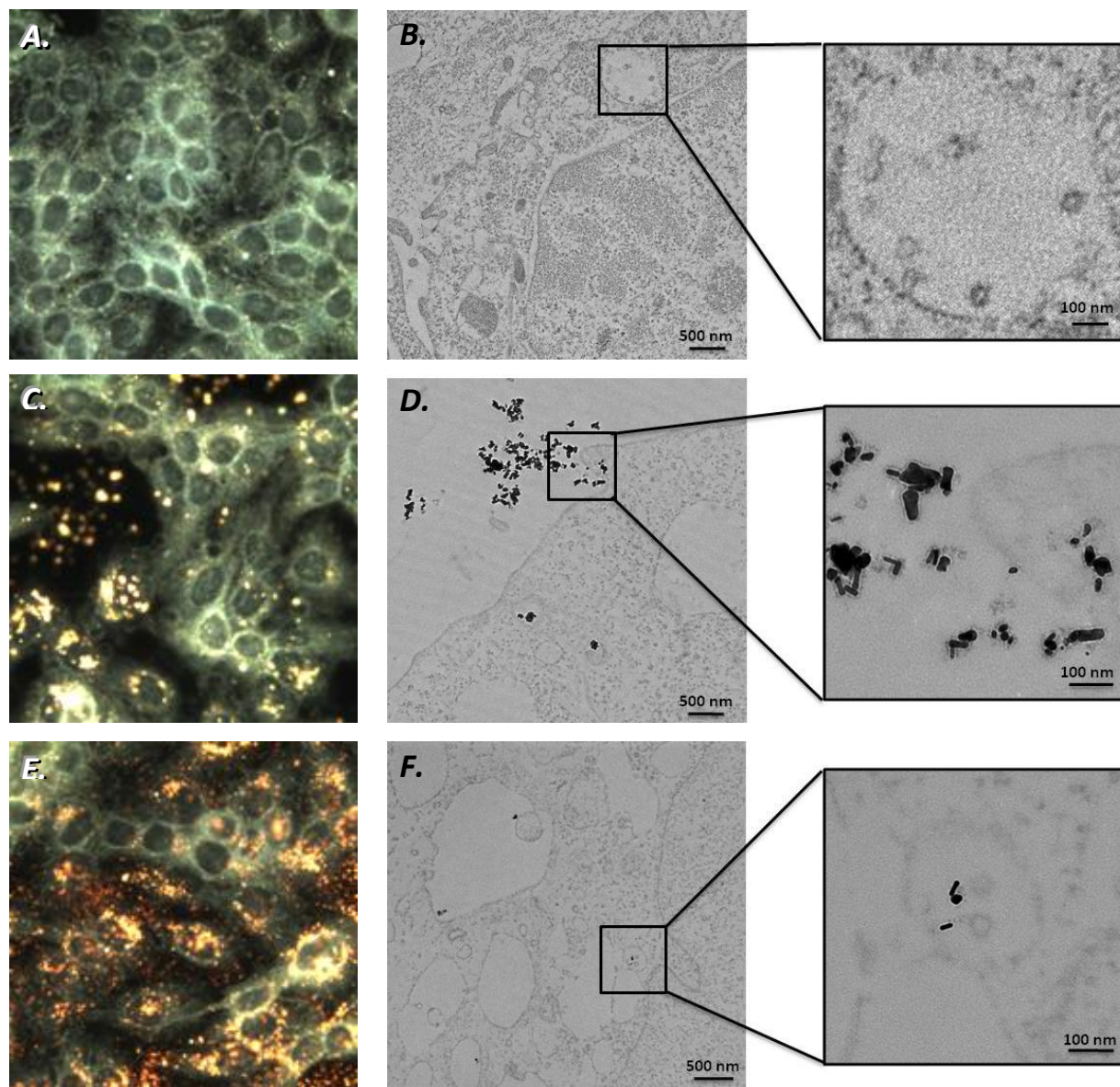


Figure 8. Cell uptake of GNR-MHDA and GNR-PEG in HaCat cells via DF imaging (A,C,E) and TEM (B,D,F). A-B. Control (no particle exposure); C-D. GNR-MHDA; E-F. GNR-PEG.

#### 4.4 Stress & Toxicity Array Analysis

RT-PCR was used to determine the effect of GNRs on HaCat cells at non-toxic doses (50 µg/mL). The Stress and Toxicity Array was used to evaluate the expression of genes directly regulated by oxidative or metabolic stress and heat shock, as well as genes that are representative of pathways activated by prolonged stress, such as apoptosis and senescence. The expression of genes was determined according to their fold regulation. Values for fold regulation from control that were greater than 3.00 were considered significant. A partial list of genes affected by GNRs are shown in Table 3.

None of the genes under review were significantly affected in cells exposed to GNR-PEG. GNR-MHDA induced up-regulation of genes associated with growth arrest, heat shock stress, inflammation, and proliferation; however, apoptotic genes were down-regulation. Genes associated with oxidative or metabolic stresses were both up and down-regulated by GNR-MHDA. DNA damage and repair genes were not significantly up- or down-regulated by any GNR exposure.

Up-regulation of genes related to inflammation, heat shock, and growth arrest indicates the cells exhibited stress responses as a result of exposure to GNR-MHDA. The most significantly affected gene was Serpine 1, which was up-regulated by a factor of nearly 9-fold more than other genes. Serpine 1 is a serine protease inhibitor, which acts by inducing the synthesis of an inhibitor protein, which inhibits the activity of tissue plasminogen activator. Plasminogen activator plays a role in cell movement and inflammation. This suggests significant inhibition of inflammation induced by exposure to GNR-MHDA after a 24 h exposure period, which may be indicative of a pro-inflammatory response that may have occurred after a shorter exposure period.

HSPH1 was the only heat shock protein-related gene of the nine that were tested in this array to be affected in cells exposed to GNR-MHDA. HSPH1 encodes a heat shock protein that prevents the aggregation of denatured proteins in cells under severe stress. Therefore, up-regulation of HSPH1 indicates the cells are under significant stress. The up-regulation of growth arrest gene GDF15 (growth differentiation factor 15), which encodes a protein that regulates



differentiation, is also likely due to cell stress (Zimmer et al., 2004). E2F1 and PCNA, genes related to proliferation and carcinogenesis, were also up-regulated by GNR-MHDA, which could be related to the proliferative effect observed by MTS data for GNR-MHDA. The down-regulation of the apoptosis related gene TNFSF10 is likely a result of an affect that occurred at a shorter time point. FMO5 encodes flavin-containing monooxygenases, which are NADPH-dependent flavoenzymes that catalyze the oxidation of heteroatom centers in drugs, pesticides, and xenobiotics. Down-regulation may indicate stress resulting from the cells trying to process GNR-MHDA that have been internalized.

The Stress and Toxicity array allows only a brief overview of gene regulation in HaCat cells exposed to GNR-MHDA. However, results from this array could be used for more in-depth analysis of the interactions of GNR-MHDA in the cells by measuring the proteins encoded by the genes and evaluating these responses at different time points.

Table 3. Genes Affected by Exposure to GNR-PEG and GNR-MHDA

Gene Symbol	Gene Type	Fold Regulation (compared to control)	
		GNR-PEG	GNR-MHDA
TNFSF10	Apoptosis Signaling	-1.60	-5.11
GDF15	Growth arrest and senescence	2.27	4.03
HSPH1	Heat shock	1.47	3.04
IL1A	Inflammation	2.23	4.32
SERPINE1	Inflammation	1.20	36.16
FMO5	Oxidative or metabolic stress	-1.67	-6.13
PTGS1	Oxidative or metabolic stress	1.84	6.87
E2F1	Proliferation and carcinogenesis	2.61	4.60
PCNA	Proliferation and carcinogenesis	1.83	6.23

## 5. SUMMARY AND CONCLUSIONS

GNR-CTAB, GNR-MHDA, and GNR-PEG induced unique responses in HaCat cells, supporting the strong influence of surface functionality on biological effects. The results of the cell viability tests showed the GNR-CTAB to be extremely toxic to the human keratinocytes. Even at the lowest dose of 5 µg/ml, only 5-10% of the cells were still viable. This observation was supported by membrane leakage assays. Both MTS and LDH results within 2 h of exposure to the GNRs, also show significant loss in cell viability and an increase in membrane leakage. However, these results were also seen after cellular exposure to the CTAB alone. This leads us to conclude that the toxicity may be due to the CTAB rather than the GNRs themselves. As CTAB is residual in GNR synthesis, it is not possible to test the toxicity of GNRs without the addition of a different stabilizing agent or functional group.

Biochemical analysis indicates that GNR-MHDA exhibited a proliferative effect on cell viability after a 24 h exposure period at low concentration (5 µg/mL) and exhibits an inhibitive effect at high concentrations (100 µg/mL). GNR-PEG only inhibited cell viability at the highest concentration (100 µg/mL). Neither GNR sample induced oxidative stress in cells after a 24 h exposure. Additional characterization was only pursued for GNR-MHDA and GNR-PEG due to the high toxicity of GNR-CTAB.

Both GNR-MHDA and GNR-PEG appear to be internalized by cells, as determined by TEM. However, the number of GNRs taken up is significantly greater for GNR-MHDA than GNR-PEG. This result is expected due to the close to neutral zeta potential of PEGylated surfaces and lack of interaction between PEGylated GNRs in biological media. Additionally, larger agglomerates of GNR-MHDA were exposed to cells, which could also play a role in the increased level of uptake.

Genetic evaluation was performed to understand the molecular and cellular interactions that may occur after exposure to GNRs. There were no effects observed after exposure to GNR-PEG. However, GNR-MHDA induced minor modulation of gene activity as a result of cell stress, which could indicate more severe toxicity for chronic exposures. Further study into the effect of GNR-MHDA on inflammation in cells is recommended. However, the difference in response at the



genetic level could likely be due to the difference in particle size of the GNR-MHDA versus GNR-PEG under cell culture conditions.

GNR-PEG shows the most promise for applications due to its high level of stability in biological media, low level of cytotoxicity, and ability to be taken up into cells. However, for applications requiring more significant cell uptake, further studies into the effect of PEG molecular weight and types of functional groups should be further investigated. For example, uptake-promoting peptides could be added to obtain both stabilizing effects of PEG as well as increased cellular uptake. Endo-lysosomal escape peptides could also be added to allow for intracellular delivery applications. Quantitative studies, such as ICP-MS, should be performed to investigate the effect of these properties on cell uptake. Further, due to the extensive agglomeration of GNR-MHDA in exposure media, it is recommended that in future studies, protein serum be present in the media used to expose GNRs to cells.

In addition to surface coating, aspect ratio (AR) must also be taken into account when studying GNRs. One study investigating the effect of AR on cytotoxicity and cellular uptake was performed by Rayavarapu et al. (2010), and it was found that PSS-coated GNRs of different ARs (2.16 and 3.72) exhibited different effects on cytotoxicity, where the shorter GNR was more cytotoxic. However, PEGylated GNRs with the same ARs did not show any toxicity effects. A more complete investigation of the effect of AR on GNR cytotoxicity is planned in future studies.

## 6. REFERENCES

- Agarwal A, Huang SW, O'Donnell M, Day KC, Day M, Kotov N, Ashkenazi SJ (2007). Targeted gold nanorod contrast agent for prostate cancer detection by photoacoustic imaging. *Appl Phys* 102, 064701.
- Alkilany AM, Nalaria PK, Hexel CR, Shaw TJ, Murphy CJ, Wyatt MD (2009). Cellular uptake and cytotoxicity of gold nanorods: Molecular origin of cytotoxicity and surface effects. *Small* 5, 701-708.
- Carlson C, Hussain SM, Schrand AM, Braydich-Stolle LK, Hess KL, Jones RL, Schlager JJ (2008). Unique cellular interaction of silver nanoparticles: Size-dependent generation of reactive oxygen species. *J Phys Chem B* 112, 13608-13619.
- Chen CC, Lin YP, Wang CW, Tzeng HC, Wu CH, Chen YC, Chen CP, Chen LC, Wu YC (2006). DNA-Gold nanorod conjugates for remote control of localized gene expression by near infrared irradiation. *J Am Chem Soc* 128, 3709–3715.
- Chithrani BD, Ghazani AA, Chan WCW (2006). Determining the size and shape dependence of gold nanoparticles uptake into mammalian cells. *Nano Lett* 6, 662-668.
- Hauck TS, Ghazani AA, Chan WCW (2008). Assessing the effect of surface chemistry on gold nanorod uptake, toxicity, and gene expression in mammalian cells. *Small* 4, 153-159.
- Huang X, El-Sayed IH, Qian W, El-Sayed MA (2006). Cancer cell imaging and photothermal therapy in the near-infrared region by using gold nanorods. *J Am Chem Soc* 128, 2115–2120.
- Huff TB, Hansen MN, Zhao Y, Cheng J, Wei A (2007). Controlling the cellular uptake of gold Nanorods. *Langmuir* 23, 1596-1599.
- Hussain S.M., Braydich-Stolle LK, Schrand AM, Murdock RC, Yu KO, Mattie DM, Schlager JJ, Terrones M (2009). Toxicity evaluation for safe use of nanomaterials: Recent achievements and technical challenges. *Adv Mater* 21, 1-11.
- Leonov AP, Zheng J, Clogston JD, Stern ST, Patri AK, Wei A (2009). Detoxification of gold nanorods by treatment with polystyrenesulfonate. *ACS Nano* 2(12), 2481-2488.
- Manohar S, Rayavarapu R, Petersen W, van Leeuwen TG (2009). Cell viability studies of PEG-thiol treated gold nanorods as optoacoustic contrast agents. *SPIE*, 7177.
- Niidome T, Yamagata M, Okamoto Y, Akiyama Y, Takahashi H, Kawano T, Katayama Y, Niidome Y (2006). PEG-modified gold nanorods with a stealth character for in vivo applications. *J Contr Rel* 114, 343-347.

Parab HJ, Chen HM, Lai TC, Huang JH, Chen PH, Liu RS, Hsiao M, Chen CH, Tsai DP, Hwu YK (2009). Biosensing, cytotoxicity, and cellular uptake studies of surface-modified gold nanorods. *J Phys Chem C* 113, 7574–7578.

Rayavarapu RG, Petersen W, Hartsuiker L, Chin P, Janssen H, van Leeuwen FWB, Otto C, Manohar S, van Leeuwen TG (2010). In vitro toxicity studies of polymer-coated gold nanorods. *Nanotechnology*, 21.

Sau TK, Murphy C J (2004). Seeded high yield synthesis of short Au nanorods in aqueous solution. *Langmuir* 20 (15), 6414-6420.

Wang S, Lu W, Tovmachenko O , Rai US, Yu H, Ray PC (2008). Challenge in understanding size and shape dependent toxicity of gold nanomaterials in human skin keratinocytes. *Chem Phys Lett* 463, 145–149.

Wijaya A, Hamad-Schifferli (2008). Ligand customization and DNA functionalization of gold nanorods via round-trip phase transfer ligand exchange. *Langmuir* 24 (18), 9966-9969.

Wijaya A, Schaffer SB, Pallares IG, Hamad-Schifferli K (2009). Selective release of multiple DNA oligonucleotides from gold nanorods. *ACS Nano* 3(1), 80-86.

Zimmers TA, Hsiao EC, Pierce RH, Jin X, McGrath SA, Chavin K, Koniaris LG (2004). Growth differentiation Factor-15/Macrophage inhibitory cytokine-1 induction through P53- and Tnf-independent mechanisms in liver, kidney, and lung injury. *J Surgical Res* 121(2), 328-329.

### **List of Symbols Abbreviations, and Acronyms**

AR	Aspect ratio
CTAB	Cetyltrimethylammonium bromide
DF	Darkfield
DLS	Dymanic light scattering
EM	Exposure media
FBS	Fetal bovine serum
GNR	Gold nanorod
HaCat	Human keratinocyte cell-line
H <sub>2</sub> O <sub>2</sub>	Hydrogen peroxide
ICP-AES	Inductively coupled plasma atomic emission spectroscopy
ICP-MS	Inductively coupled plasma mass spectrometry
LDH	Lactate dehydrogenase
MHDA	Mercaptohexadecanoic acid
MS	Mass spectroscopy
MTS	3-(4, 5-dimethylthiazol-2-yl)-5-(3-carboxymethoxyphenyl)-2-(4-sulfophenyl)-2H-tetrazolium, inner salt
mV	Millivolts
NIR	Near infrared
ng	Nanogram
nm	Nanometer
PAA	Polyacrylic acid
PAH	Polyelectrolyte poly(allylamine) hydrochloride
PBS	Phosphate buffered saline
PDADMAC	Poly(diallyldimethyl ammonium chloride
PEG	Polyethylene glycol
Pen/strep	Penicillin/streptomycin
PSS	Polys(4-styrene sulfonic acid)
ROS	Reactive oxygen species
RT-PCR	Reverse transcriptase polymerase chain reaction
TEM	Transmission electron microscopy
UV/VIS	Ultraviolet/Visible spectroscopy
μ	Micro
μL	Microliter
μm	Micrometer

